Facile preparation of Zn@CNF for high-stability zinc anodes

Ye Zhang [1, a], Yi Jiang [2, b], Guixia Liu [1, c, *]

[1] School of Chemistry and Environmental Engineering, Changchun University of Science and Technology, Changchun, China.

[2] School of Science, Changchun Institute of Technology, Changchun,130012, China

[a] 670189877@qq.com, [b] jiangyi@ccit.edu.cn, [c] liuguixia22@163.com

Abstract. Aqueous zinc-ion batteries (AZIBs) are renowned for their exceptional safety and eco-friendly design, are being considered as a prospective option for emerging energy storage technologies. However, the selected Zn foil as the anode material in existing AZIBs encounters significant challenges, including dendrite formation due to uneven zinc deposition/stripping, and undesirable side reactions. These issues considerably degrade the lifespan and capacity of the battery, thereby impeding its practical application and commercialization. To address these problems, this research introduces a highly stable Zn@CNF anode for AZIBs by using carboxylated cellulose nanofibers (CNFs) as a protective coating. Under consistent testing conditions, the symmetric batteries of Zn@CNF maintain stable Zn deposition/stripping behavior for 500 h, while the unprotected Zn symmetric batteries fail after merely 100 h. Additionally, during full-cell evaluations, the Zn@CNF||MnO_2 batteries increase capacity compared to Zn||MnO_2 battery. This approach offers a practical way for developing highly stable Zn anodes.

Keywords: Zinc ion battery, anode, Zn@CNF.

1. Introduction

The accelerated development of renewable energy technologies and mobile electronics has driven significant demand for economical and reliable electrochemical storage systems [1]. Among emerging alternatives, aqueous zinc-ion batteries (AZIBs) stand out as a viable option for advanced energy storage system, distinguished by their high theoretical capacity (820 mAh g^{-1}, 5855 mAh cm^{-3}), cost-efficient fabrication processes, and superior operational safety compared to conventional organic electrolyte-based battery systems [2,3]. Nevertheless, critical challenges persist regarding the Zn metal anode in AZIBs configurations, particularly concerning uncontrolled dendritic crystallization and parasitic hydrogen evolution reactions (HER), which collectively deteriorate electrochemical performance and operational durability [4-6]. Addressing these fundamental limitations through advanced anode engineering strategies represents a crucial pathway toward realizing the full potential of AZIBs technology in practical energy storage applications.

Currently, researchers mainly improve the stability of Zn anode by surface modification [7-9], electrolyte engineering [10-12] and adjusting the separator [13, 14]. Regarding surface modification, surface engineering of Zn anodes via coating or spraying techniques offers a straightforward method to establish a protective layer, thereby enhancing anode stability. However, this method mostly relies on first synthesizing the protective layer material, then mixing it with binder and organic solvent to form a slurry and subsequently coating or spraying it onto the Zn anode to prepare the Zn anode with the protective layer. This process may involve complex synthesis methods and the organic solvents used in the process are not environmentally friendly. Therefore, designing a high-stability Zn anode using simple and environmentally friendly methods remains a challenge.

Herein, Zn@CNF for AZIBs anodes was fabricated by spraying a dispersion liquid of carboxylated cellulose nanofibers (CNFs) onto Zn foil and subsequently drying it. The Zn@CNF demonstrates exceptional stability, with its symmetric batteries showing a significantly extended cycle life in comparison to the conventional bare Zn symmetric batteries. This enhancement in stability is ascribed to the carboxyl groups within the CNFs, which facilitate the desolvation of hydrated zinc ions, as well as the interfacial barrier effect provided by the protective layer.

Moreover, during the performance evaluations of the full cells, Zn@CNF||MnO_2 exhibited superior results in comparison to Zn||MnO_2.

2. Experiment

2.1 Materials

Zn foil with thickness 0.05 mm and stainless steel (SS) foil with thickness 0.02 mm (Hefei Wenghou Metal Material, 99.99%), carboxylated cellulose nanofibers (CNFs, Shanghai Macklin Biochemical Co., Ltd.), polyvinylidene fluoride (PVDF), potassium permanganate ($KMnO_4$) and hydrogen chloride (HCl) (Sinopharm Chemical Reagent Co., Ltd.), zinc sulfate ($ZnSO_4 \cdot 7H_2O$) and manganous sulfate ($MnSO_4 \cdot 4H_2O$) (Aladdin Chemistry Co., Ltd.). super P (Guangzhou Candle New Energy Technology Co., Ltd.).

2.2 Preparation of Zn@CNF anode

The 1 wt% CNF dispersion was prepared and homogenized using ultrasonic agitation. The Zn foil (12 mm diameter) was spray-coated with the dispersion and dried at 50 °C for 12 h, yielding the Zn@CNF composite.

2.3 Preparation of MnO_2 cathode

The MnO_2 cathode synthesis employed a modified hydrothermal protocol adapted from established methodologies [15]. During the synthesis process, A solution of 0.8 g $KMnO_4$ in 50 mL DI water was prepared by continuous stirring until complete dissolution. After introducing 2 mL HCl into the homogeneous solution, the mixture underwent 5 minutes of vigorous agitation. The mixture was introduced into a autoclave for hydrothermal crystallization at 140°C for 12 h. The resultant precipitate underwent sequential purification through three cycles of centrifugation (3000 rpm, 5 min) via sequential purification with DI water and anhydrous ethanol prior to 12 h vacuum desiccation (60°C). For electrode fabrication, active material (MnO_2), conductive carbon (Super P), and polymeric binder (PVDF) were homogeneously blended in a 7:2:1 mass ratio using NMP as the dispersion medium. The formulated slurry was doctor-bladed onto 316L stainless steel substrates and thermally cured at 80°C for 24 h. Through sequential optimization of the coating process, the electrode's mass loading was carefully regulated within the range of 1.0-1.3 mg cm^{-2}.

2.4 Characterizations

Crystalline phase analysis was conducted via a Rigaku D/max-RA diffractometer employing Cu Kα irradiation (λ=0.15406 nm). SEM-imaged surface features and EDS-based compositional mapping were performed using a JEOL JSM-7610F field-emission SEM system equipped with an Oxford ISIS-300 EDS detector.

2.5 Electrochemical measurements

For constructing symmetric and full cells architectures, CR2025 coin cells were adopted as electrochemical containers utilizing Whatman GF/D glass fiber separators The symmetric cell system utilized a 2 M $ZnSO_4$ aqueous electrolyte, while the full cells configuration incorporated a composite electrolyte of $ZnSO_4$ -$MnSO_4$ (0.2 M $MnSO_4$ additive). Batteries performance tests were conducted under ambient conditions using Land CT3002A. Cyclic voltammetry measurements (0.9 - 1.8 V, 0.1 mV s-1) were executed on a CHI660E. Linear sweep voltammetry (1 mV s-1) and Tafel polarization (1 mV s-1) analyses were performed in a standard three-electrode system, employing bare Zn and Zn@CNF as working electrodes, Pt foil as the counter electrode, and Ag/AgCl as the reference electrode.

3. Results and Discussion

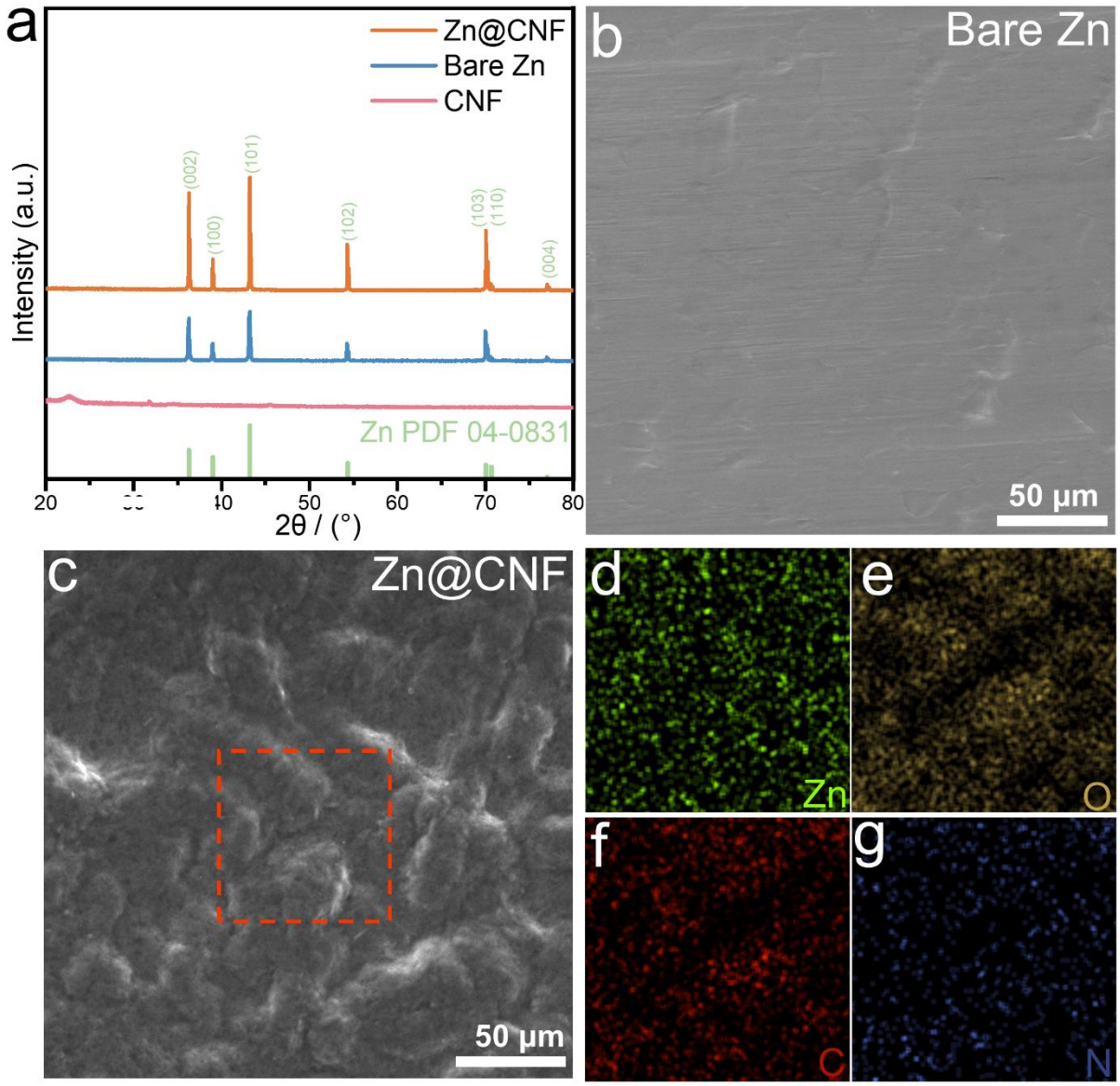

Fig. 1 (a) XRD patterns of Zn@CNF, bare Zn and CNF. SEM images of (b) bare Zn and (c) Zn@CNF. (d-g) Corresponding elemental mappings of Zn@CNF.

Fig. 1a shows the XRD patterns of Zn@CNF, bare Zn and CNFs. The phenomenon that no diffraction peaks belonging to CNFs exist in Zn@CNF can be ascribed to the protective layer formed by CNFs on the sprayed surface being too thin. Figs. 1b and 1c are the SEM images of bare Zn and Zn@CNF respectively. The obvious change in morphology indicates that the protective layer of CNFs has been successfully uniformly attached to the Zn foil. Figs. 1d-g are the corresponding element distribution diagrams of the boxed areas in Fig. 1c. It is evident that, apart from the Zn element, the elements of C, O and N belonging to CNFs have also been detected. These experimental findings demonstrate the successful formation of CNFs interfacial coatings on zinc substrates through a facile spray-deposition method.

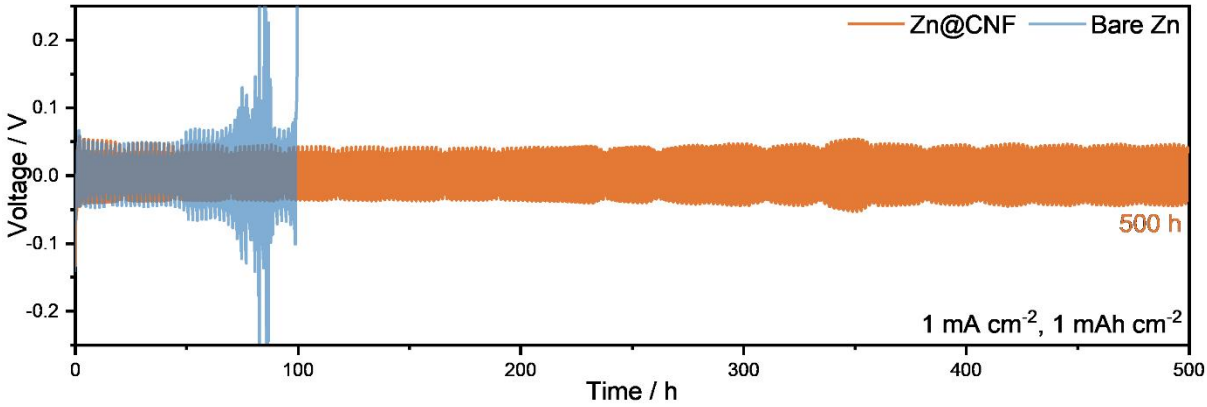

Fig. 2 The stability tests of bare Zn and Zn@CNF in the symmetric batteries.

The electrochemical stability of Zn@CNF and bare Zn was comparatively investigated through symmetric celsl with galvanostatic cycling characterization (Fig. 2). As observed, the voltage of the bare Zn symmetric cells exhibited a marked increase at 50 h, which is attributed to the non-uniform electroplating/stripping behavior of Zn. With the continuous progression of this non-uniform deposition/stripping process, the bare Zn symmetric cells fail at 100 h. In contrast, the Zn@CNF symmetric cells exhibit stable cycling performance over 500 h. This enhanced stability can be ascribed to the carboxyl groups in the protective layer, thereby accelerating the stripping of solvation shells from Zn^{2+} species, thus allowing for even Zn deposition and enhancing the overall performance of the symmetric cells.

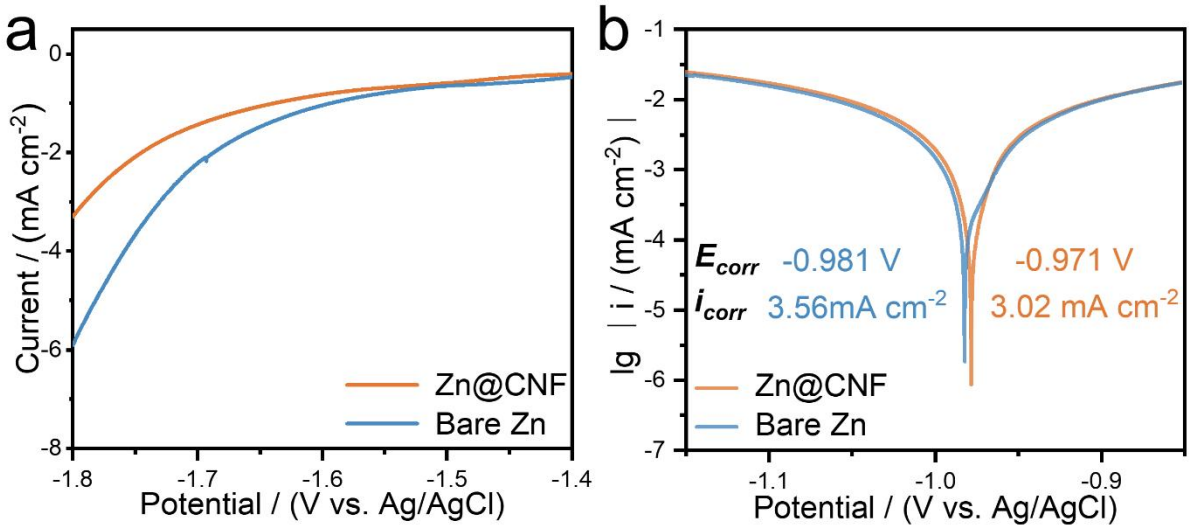

Fig. 3 (a) Inhibitory ability of HER tests of bare Zn and Zn@CNF in 1 M Na_2SO_4. (b) The corrosion resistance tests of bare Zn and Zn@CNF in 2 M $ZnSO_4$.

The inhibitory capability of Zn@CNF and bare Zn in suppressing HER was assessed using LSV curves tests. It can be seen that the curve of Zn@CNF consistently remains above that of bare Zn (Fig. 3a). This result indicates that, under the same voltage, the current density associated with Zn@CNF is lower. Consequently, Zn@CNF demonstrates better HER suppression performance in comparison to bare Zn. Fig. 3b displays the linear polarization curves of Zn@CNF and bare Zn for evaluating corrosion resistance. Experimental data demonstrate that Zn@CNF exhibits a nobler corrosion potential (-0.971 V) and reduced corrosion current (3.02 mA cm^{-2}) relative to unprotected zinc (-0.981 V, 3.56 mA cm^{-2}), confirming improved anti-corrosion properties in the composite material.

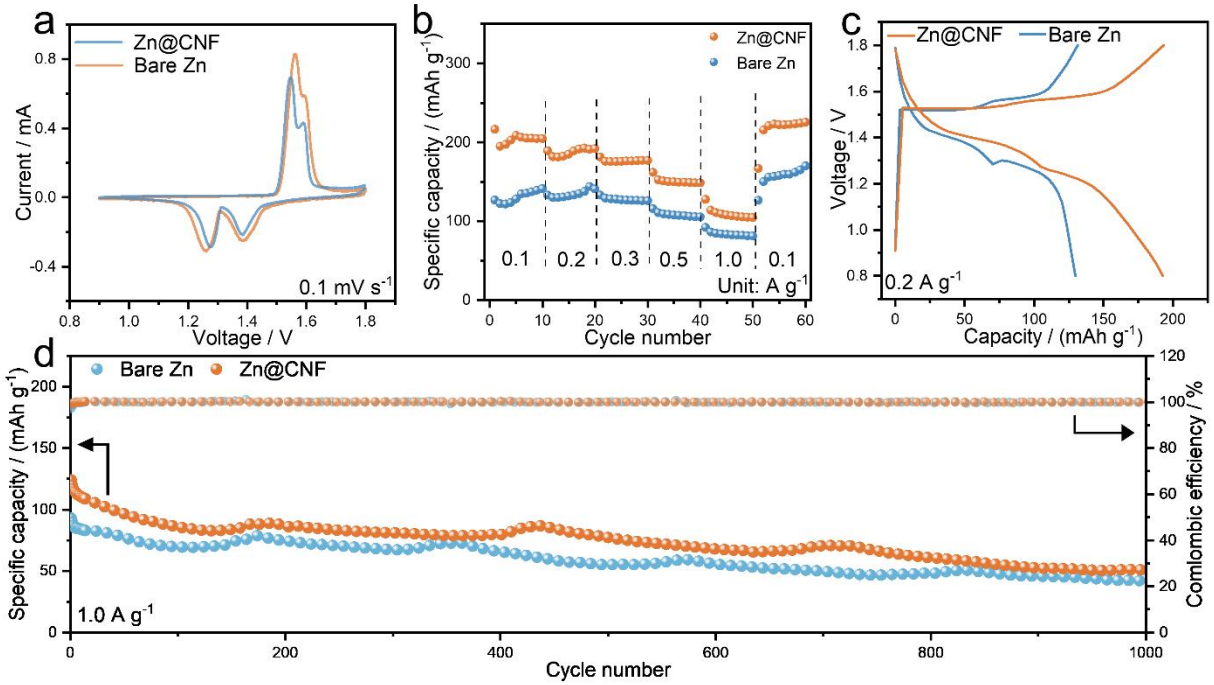

Fig. 4 (a) CV curves, (b) rate performance, (c) charge/discharge curves at 0.2 A g^{-1}, (d) cyclic test under high current density at 1.0 A g^{-1} of Zn@CNF||MnO_2 and Zn||MnO_2 cells.

In practical applications, Zn@CNF and bare Zn were employed as the anodes, while MnO_2 served as the cathode of full cells for testing. From the CV curves of Zn||MnO_2 and Zn@CNF||MnO_2 (Fig. 4a), it exhibits greater oxidation/reduction peaks for Zn@CNF||MnO_2 relative to Zn||MnO_2, indicating superior chemical reversibility and higher capacity [16]. Fig. 4b illustrates the rate performance of Zn||MnO_2 and Zn@CNF||MnO_2. Under different current densities, Zn@CNF||MnO_2 consistently demonstrates a higher capacity. Furthermore, both systems exhibit excellent capacity recovery after high current density tests, highlighting their outstanding reversibility. At 0.2 A g^{-1}, the Zn@CNF||MnO_2 achieves 192.7 mAh g^{-1}, which is 48.6% higher than that of Zn||MnO_2 (129.7 mAh g^{-1}) (Fig. 4c). After 1000-cycle operation at 1.0 A g^{-1}, Zn@CNF||MnO_2 maintains a higher capacity than Zn||MnO_2 (Fig. 4d). The aforementioned findings suggest that Zn@CNF anode material has advantages in practical applications.

4. Summary

In conclusion, we successfully fabricated a CNFs protective layer on Zn foil via a simple and environmentally friendly approach to develop the Zn@CNF anode material for aqueous zinc-ion batteries (AZIBs). The carboxyl groups within CNFs are capable of efficiently enhancing the de-solvation of hydrated Zn ions, facilitating uniform Zn deposition while inhibiting dendrite formation. Functioning as the barrier, the CNF interphase effectively isolates zinc anodes from bulk electrolyte, thereby suppressing associated side reactions. Consequently, the Zn@CNF symmetric batteries achieve superior cycle durability over 500 h, whereas the bare Zn symmetric batteries fail after only 100 h. Moreover, the Zn@CNF||MnO_2 configuration demonstrates a 48.6% capacity enhancement over conventional Zn||MnO_2 (192.7 vs. 129.7 mAh g^{-1}) at 0.2 A g^{-1}. Despite undergoing 1000 cycles at 1.0 A g^{-1}, the Zn@CNF||MnO_2 cells retain its capacity advantage. This simple method for preparing stable Zn anode will further promote the application of AZIBs.

Acknowledgements

This study was supported financially by the Science and Technology Development Planning Project of Jilin Province (20240101075JC).

Conflicts of Interest

The authors declare no conflicts of interest regarding the publication of this paper.

References

[1] Zhang Mengyun, Wang Li, Xu Hong, et al. Polyimides as promising materials for lithium-ion batteries: a review. Nano-Micro Letters, 2023, 15(1): 135.

[2] Liu Xiaoqi, Zhang Yu, Wang Liying, et al. Highly reversible dendrite-free zinc anode enabled by a bilayered inorganic-metal interface layer. ACS nano, 2024, 18(52): 35325-35335.

[3] Pu Yujuan, Zhang Youkui, Zhan Kaiyuan, et al. Fast kinetics enabled by ion enrichment layer for dendrite-free zinc anode. Small Methods, 2024: 2401936.

[4] Li Bin, Liu Shude, Geng Yifei, et al. Achieving stable zinc metal anode via polyaniline interface regulation of Zn ion flux and desolvation. Advanced Functional Materials, 2024, 34(5): 2214033.

[5] Lin Dewu, Shi Dehuan, Zhu Anquan, et al. Self-adaptive hierarchical hosts with switchable repulsive shielding for dendrite-free zinc-ion batteries. Advanced Energy Materials, 2024, 14(14): 2470059.

[6] Xing Zhenyue, Sun Yanyan, Xie Xuesong, et al. Zincophilic electrode interphase with appended proton reservoir ability stabilizes Zn metal anodes. Angewandte Chemie International Edition, 2023, 62 (5): e202215324.

[7] Li Li, Yang Hang, Yuan Zeyu, et al. The organic ligand etching method for constructing in situ terraced protective layer toward stable aqueous Zn anode. Small, 2023, 19(52): 2305554.

[8] Tian Siyu, Zhou Long, He Wei, et al. A self-assembled nanoporous polyelectrolytic interlayer for highly stable zinc metal anodes. Chemical Engineering Journal, 2023, 462: 142276.

[9] Dong Haobo, Hu Xueying, Liu Ruirui, et al. Bio-inspired polyanionic electrolytes for highly stable zinc-ion batteries. Angewandte Chemie International Edition, 2023, 135(41): e202311268.

[10] Wang Yanyan, Wang Zhijie, Pang Wei Kong, et al. Solvent control of water O−H bonds for highly reversible zinc ion batteries. Nature Communications, 2023, 14(1): 2720.

[11] Ouyang Kefeng, Chen Sheng, Ling Wei, et al. Synergistic modulation of in-situ hybrid interface construction and pH buffering enabled ultra-stable zinc anode at high current density and areal capacity. Angewandte Chemie International Edition, 2023, 62(45): e202311988.

[12] Wang Fei, Borodin Oleg, Gao Tao, et al. Highly reversible zinc metal anode for aqueous batteries. Nature materials, 2018, 17(6): 543-549.

[13] Bu Fanxing, Sun Zhihao, Zhou Wanhai, et al. Reviving Zn0 dendrites to electroactive Zn2+ by mesoporous MXene with active edge sites. Journal of the American Chemical Society, 2023, 145(44): 24284-24293.

[14] Li Chao, Sun Zhongti, Yang Tian, et al. Directly grown vertical graphene carpets as janus separators toward stabilized Zn metal anodes. Advanced Materials, 2020, 32(33): 2003425.

[15] Liu Sang-Sang, Liang Ya-Ru, Chen Wen-Long, et al. Ultrathin surface coating of Cu enabling long-life Zn metal anodes. Rare Metals, 2024, 43(5): 2125-2135.

[16] Zhang Ye, Yan Kai, Jiang Yi, et al. Long-life and highly stable Zn metal anodes achieved by Ag nano-coating via electron beam evaporation. Chemical Engineering Journal, 2024, 502: 157933.